NUMERICAL ASSESSMENT OF PARCEL MODELING IN LARGE EDDY SIMULATION FOR DISPERSED MULTIPHASE FLOWS

L. Bahramian, F.X. Trias, C. Oliet and C.D. Pérez-Segarra

Heat and Mass Transfer Technological Center, Technical University of Catalonia
Carrer de Colom 11, 08222 Terrassa (Barcelona), Spain; www.cttc.upc.edu
{*linda.bahramian, francesc.xavier.trias, carles.oliet, cdavid.perez.segarra*}*@upc.edu*

Abstract

The particle-laden turbulent flow benchmark case of a confined jet by Hishida (1987) was selected for validation purposes of the Eulerian-Lagrangian method in Large Eddy Simulation (LES). After validation, a particle size distribution was determined and the streamwise particle velocities in three different parcel models were studied; the Number Fixed Model (NFM), the Volume Fixed Model (VFM) and the hybrid parcel model, a combination of these two previous models. The purpose behind introducing a new hybrid parcel model was to optimize the computational cost of the simulation versus the accuracy. Results show that this hybrid model presents better agreement and fewer discrepancies in the mean and the Root Mean Square (RMS) velocity profiles for the small particle diameters compared to the VFM and also for the large particle diameters compared to the NFM. In the next step, a Langevin stochastic model for subgrid dispersion of Lagrangian particles was implemented to analyze its effect on the particle turbulent statistics. For this purpose, the subgrid Stokes number of different classes of particles was analyzed to shed more light on the impact of using the stochastic subgrid model for this case. It has shown that the effect of the applied stochastic subgrid model in the RMS velocities of the dispersed phase of the current case was negligible.

1 Introduction

Dispersed multiphase flow plays an essential role in various applications such as aircraft icing, fuel injection in the combustion chamber, dispersion of pollutants, evaporative cooling, cyclone separators, inertial particle separators, etc. One of the approaches to deal with the numerical simulation of dispersed multiphase flows is the Eulerian-Lagrangian approach (explained in detail in the work of Subramaniam (2013)), where thousands or millions of particles are present in the domain. The Eulerian part is used for the fluid simulation, and the Lagrangian method is used for tracking the dispersed phase.

For industrial applications where a large domain is applied, tracking millions of particles needs huge computational resources. Using the parcel method is one approach for decreasing the computational cost besides having reasonable accuracy. A parcel is a group of particles with similar characteristics, such as diameter and velocity. The two standard models used for parcel modeling are the NFM and the VFM, which are presented in the work of Watanabe et al. (2015). In order to enhance the computational cost versus accuracy in a wide range of particle diameter distribution, a combined model has been presented, which is explained in detail in the work of Bahramian et al. (2022). The first goal is to dig into more detail about the parcel models and study their behaviors through different simulation conditions using the polydispersed two-phase flows.

M. Kuerten (2016) presented a review of numerical simulation methods for point-particle Direct Numerical Simulation (DNS) and LES of particle-laden turbulent flows. One of the common numerical simulation methods used in particle-laden turbulent flows is LES, where the large scales of the flow are well-resolved, and the subgrid scales (SGS) are modeled. An essential aspect in the development of this numerical method for dispersed multiphase flows is to evaluate and investigate the effect and importance of the SGS on the dispersed phase. This effect can be neglected when there is a low residual energy content in the desired regions of the computational domain. Otherwise, the influence of SGS effects on the Lagrangian particles should be considered. Fede and Simonin (2006) investigated the effects of SGS on the motion of non-settling colliding particles in a steady homogeneous isotropic turbulent flow. They showed that the particle turbulent dispersion and kinetic energy are impacted by the filtering only when a significant amount of the turbulent kinetic energy was extracted from the velocity field seen by the particles.

2 Mathematical formulations

In this section, the essential equations that have been applied are summarized. The dispersed phase motion in a continuous phase using a Lagrangian method can be defined by Newton's law. The primary work in this field was carried out by Basset (1888), Boussinesq (1885) and Oseen (1927), called BBO-equation. The BBO-equation in non-uniform flow for small rigid particles was studied in detail by Maxey and Riley (1983).

Therefore, the governing equations for determining the nth particle position and momentum are:

$$\frac{\mathrm{d}\mathbf{x_p^n}}{\mathrm{d}t} = \mathbf{v_p^n} \tag{1}$$

$$m_\mathrm{p}^n \frac{\mathrm{d}\mathbf{v_p^n}}{\mathrm{d}t} = \sum_i \mathbf{F_i} \tag{2}$$

where $\mathbf{x_p^n}$, $\mathbf{v_p^n}$, and m_p^n are the nth particle's center location, velocity, and mass. The sum of forces appearing on the right-hand side of Eq. (2) accounts for all the relevant forces acting over the particles, e.g., drag, gravity, added mass, pressure gradient force, etc. It is assumed that particles are large enough that any Brownian or non-continuum motion of the particles may be neglected.

Eq. (2) under influence of drag and buoyancy forces can be expressed as:

$$\begin{aligned} m_\mathrm{p}^n \frac{\mathrm{d}\mathbf{v_p^n}}{\mathrm{d}t} = \frac{1}{2}\rho_\mathrm{c} C_D A_\mathrm{p}^n \left|\mathbf{u}(\mathbf{x_p^n}) - \mathbf{v_p^n}(\mathbf{x_p^n})\right| \\ \left(\mathbf{u}(\mathbf{x_p^n}) - \mathbf{v_p^n}(\mathbf{x_p^n})\right) + \left(1 - \frac{\rho_\mathrm{c}}{\rho_\mathrm{p}}\right) m_\mathrm{p}^n \mathbf{g} \end{aligned} \tag{3}$$

where ρ_c and ρ_p are the density of the fluid (assumed constant) and the density of the particle. C_D is the drag coefficient, A_p^n, the particle cross-section area, $\mathbf{g}$, gravitational acceleration vector and $\mathbf{u}(\mathbf{x_p^n})$ is the fluid's velocity at the nth particle's position.

The drag force is assumed to be the only significant fluid-particle interaction force in the particle-fluid two-way coupling. The Navier-Stokes (NS) equations govern the behavior of viscous incompressible continuous fluids, which is detailed in the work of Sagaut (2005). They can be approximated by:

$$\nabla \cdot \ \mathbf{u} = 0 \tag{4}$$

$$\rho_\mathrm{c}\left[\frac{\partial \mathbf{u}}{\partial t} + \nabla \cdot (\mathbf{u}\mathbf{u})\right] = -\nabla p + \mu \nabla^2 \mathbf{u} + \mathbf{S_u} \tag{5}$$

$$\mathbf{S_u} = -\sum_{n=1}^{N_\mathrm{p}} \frac{m_\mathrm{p}^n \mathbf{f_{cp}^n}}{V_\mathrm{cell}} \tag{6}$$

where p, μ, and $\mathbf{S_u}$ are the pressure, the dynamic viscosity, and the momentum source term. $\mathbf{f_{cp}^n}$, V_cell, and N_p are the fluid-particle interaction force per unit mass of the particle, the volume of the computational cell, and the number of particles occupying in a computational cell.

3 Results and Discussion

The selected benchmark test case is the confined jet of Hishida (1987) which is shown in Figure 1. It is a vertical descending jet injecting particles in the center zone of it. The configuration includes two concentric cylinders, an injector and a pipe. The flow is turbulent, isothermal and incompressible. All the numerical simulations have been carried out through an in-house parallel C++/MPI CFD code called TermoFluids based on the finite volume method (FVM) and symmetry-preserving discretization of NS equations on unstructured collocated grids Trias et al. (2014).

Validation

In order to validate the numerical simulation, the heavy particle distribution of the benchmark case of Hishida (1987) with particle diameters of 64.4 μm and density of 2590 kg/m^3 is selected. This simulation is carried out by tracking all the particles (no parcel modeling). Figures 2, 3, 4 and 5 show the radial profiles of the mean and the RMS streamwise velocities of the carrier and the dispersed phase in different sections of the domain perpendicular to the direction of the flow. As can be seen, the numerical simulation follows the experimental data both for the fluid and the dispersed phase in good agreement.

Designing the hybrid parcel model

In order to investigate the different parcel models, a particle size distribution is determined. Here the particles are ordered with the mean diameter class of 20, 30, 40, 50, 60, 70, 80, 90, 100μm and the Sauter Mean Diameter (SMD) of 60 μm (the SMD calculation defined in the work of Azzopardi (2011)). Different number of particles per parcel is examined in the NFM to decide the appropriate number of particles per parcel for the SMD. The hybrid model can be set by determining the number of particles per parcel for the SMD, as shown in Table 1. Determining the number of particles per parcel for the SMD has been described in more detail in the work of Bahramian et al. (2022). In

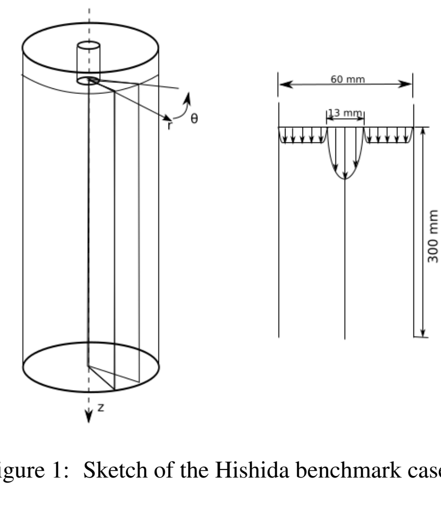

Figure 1: Sketch of the Hishida benchmark case.

this model, the particle diameter class above the SMD is arranged by the VFM and the particle diameter class below the SMD is set by the NFM. After analyzing the results, the number of particles per parcel for the SMD has been set to 15. According to Table 1, the particle classes using the NFM will have the same number of particles per parcel as the SMD and the ones using the VFM will have the same volume as the SMD parcel.

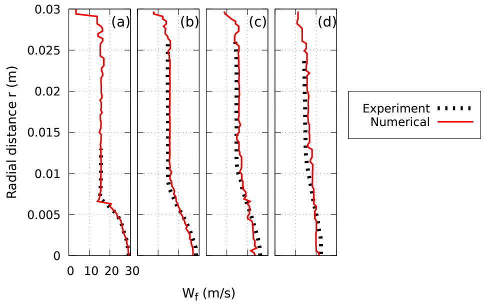

Figure 2: Radial profiles of fluid mean streamwise velocity for Hishida benchmark case. Circle: Experiment; solid line: Numerical simulation. (a) z=0m; (b) z=0.065m; (c) z=0.13m; (d) z=0.26m.

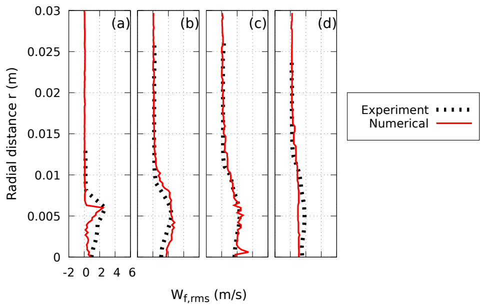

Figure 3: Radial profiles of fluid RMS streamwise velocity for Hishida benchmark case. Circle: Experiment; solid line: Numerical simulation. (a) z=0m; (b) z=0.065m; (c) z=0.13m; (d) z=0.26m.

Table 1: Defining the hybrid parcel model according to particle diameter distribution

dp(μm)	20	30	40	50
Parcel Type	NFM	NFM	NFM	NFM
dp(μm)	70	80	90	100
Parcel Type	VFM	VFM	VFM	VFM

Comparision of parcel models

Figures 6, 7, 8 and 9 show the streamwise profiles of particle mean and RMS velocity at r=0 for two different particle diameters(one small and one large classes of particle). The objective here was to see if the hybrid model could present better behavior than the VFM for the particles with diameters smaller than the SMD and show fewer discrepancies than the NFM for the particles with diameters above the SMD. As can be seen in Figures 6 and 8, the hybrid model follows the no-parcel model properly, but the VFM shows some discrepancies in both the mean and the RMS velocity profiles. The zero velocities signify that there is no parcel in that location, so it does not show good dispersion for small diameter classes of particles, especially at the beginning of the streamwise direction at the center line. Figures 7 and 9 show that the hybrid model is tracking the values of the no-parcel model appropriately both for the mean and the RMS velocity profiles, but the NFM shows some discrepancies and also presents zero velocities at the beginning of the domain. It signifies that there is no parcel with particle diameters of 80 μm at the beginning of the streamwise direction at the center-line, showing no proper dispersion for the large particles.

After this comparison, the effect of the SGS on the RMS velocities of Lagrangian particles has been stud-

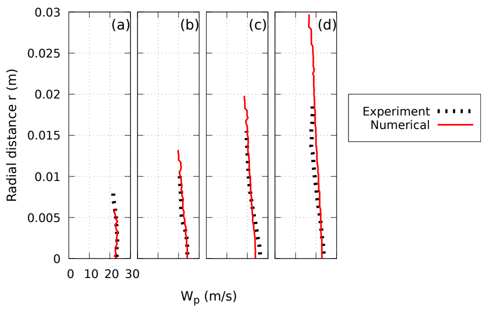

Figure 4: Radial profiles of particle mean streamwise velocity for Hishida Benchmark case. Circle: Experiment; solid line: Numerical simulation. (a) z=0m; (b) z=0.065m; (c) z=0.13m; (d) z=0.26m.

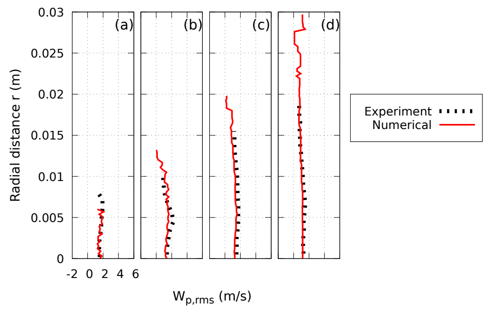

Figure 5: Radial profiles of particle RMS streamwise velocity for Hishida Benchmark case. Circle: Experiment; solid line: Numerical simulation. (a) z=0m; (b) z=0.065m; (c) z=0.13m; (d) z=0.26m.

ied. For this purpose, the stochastic model proposed by Bini and Jones (BJ) (2007,2008) is implemented, where the Langevin type equation is applied to the particle velocity. The results are presented in Figures 10, 11, 12, 13. These Figures show the streamwise RMS velocity profiles of the no-parcel model and the hybrid model with and without the stochastic subgrid model for two particle class diameters of $dp = 20\mu m$ and $dp = 80\mu m$. As can be seen by implementing this stochastic subgrid model, the differences between the RMS velocities of the particles are negligible.

Figures 14 and 15 display subgrid Stokes number in streamwise direction for particle classes of $dp = 20\mu m$ and $dp = 80\mu m$. Solid particles can generally sense turbulence with time scales smaller than their response times. This can be measured using the subgrid Stokes number, which is defined as the ratio of the particle response time to the subgrid turbulence time scale, which is discussed comprehensively in the work of Berrouk (2012). As can be seen in this Figures, the subgrid Stokes number of particles can vary depending on the location of the particles in the domain. Regarding this Figures, the class of particles with $dp = 20\mu m$ cannot sense some of the turbulence in the second mid in the streamwise direction where their Stokes numbers based on the subgrid time scale are smaller than one. This is caused by coarsening the mesh in this area, where a stochastic subgrid model for this class of particles can be applied. Although seems the class of particles with $dp = 80\mu m$ can sense almost all the turbulence in this streamwise direction. That could be the reason where applying a stochastic subgrid model is not showing significant changes in the RMS velocity of these two different classes of particles. The Broader analyses of the subgrid Stokes number for all particle classes are needed in the streamwise and radial direction for a more comprehensive conclusion regarding the stochastic subgrid effect.

4 Conclusions

The current study is centered around the development of a novel approach for parcel modeling, achieved through a combination of the NFM and the VFM based on the SMD and the effect of the stochastic SGS on the particle turbulent characteristics. The numerical results for radial profiles of streamwise velocities of both the continuous and dispersed phases demonstrate good agreement with experimental findings. The hybrid parcel model is designed based on the SMD, utilizing the NFM for particle diameters below the SMD and the VFM for diameters above it. Compared to the VFM, the hybrid model improved the parcel dispersion and reduced the discrepancies in the mean and the RMS velocity profiles of the dispersed phase for the particle diameters below the SMD. Considering the results of the NFM, the hybrid model exhibits better agreement and fewer discrepancies in the mean and the RMS velocity profiles of the dispersed phase for particle diameters above the SMD. In conclusion, the preliminary results of the hybrid parcel model, when compared to the previous models (the NFM and the VFM), maintain an appropriate level of accuracy and particle dispersion. Further analyses concerning the quantities of the particle dispersion, computational costs and particle volume fraction will be conducted for the hybrid model.

In the next step, a stochastic subgrid model is studied on the RMS velocities of particles for no-parcel and the hybrid model. Upon implementing this stochastic model, only minor differences are observed in the RMS velocities of the particles. It was observed that the values of the subgrid Stokes numbers of two different classes of particles (one small and one large particle class diameter) were above one in the majority of the streamwise direction. It leads to the conclusion that almost all particle classes can sense the majority of turbulence in the streamwise direction. Therefore, the effects of the applied stochastic subgrid model with this particle size distribution and density through this mesh configuration can be negligible on the RMS velocities of the dispersed phase in the streamwise direction. Further in-depth analyses of the particle subgrid Stokes number, different stochastic subgrid models, and mesh sensibility will be required to draw more comprehensive conclusions for the stochastic subgrid effects on particle characteristics.

Acknowledgments

This work has been developed within the EU H2020 Clean Sky 2 research project "A New proTection devIce for FOD - ANTIFOD" (grant agreement Nº 821352).

Linda Bahramian acknowledges the financial support from the Secretariat of Universities and Research of the Generalitat de Catalunya and the European Social Fund, FI AGAUR Grant (2019 FI_B 01205) and the UPC-Santander Grant. Carles Oliet, as a Serra Húnter associate professor, acknowledges the Catalan Government for the support through this Programme.

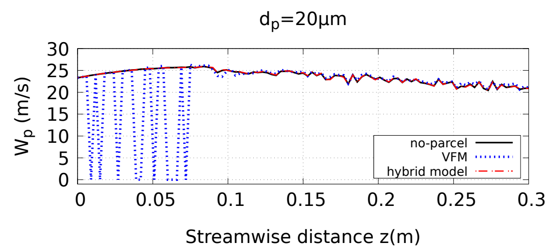

Figure 6: Streamwise profiles of particle mean velocity ($dp = 20\mu m$) for the Hishida configuration comparing no-parcel, VFM and hybrid model.

References

Azzopardi, B.J. (2011), Sauter mean diameter. *Thermopedia, [Online]. Available: http://www.thermopedia.com/content/1108/. [Accessed 01 03 2013].*

Bahramian, L., Muela, J., Oliet, C., Pérez-Segarra, C.D. and Trias, F.X. (2022), An Efficient Strategy of Parcel Modeling for Polydispersed Multiphase Turbulent Flows. *World Congress in Computational Mechanics and ECCOMAS Congress*

Basset, A.B. (1888), On the motion of a sphere in a viscous liquid. *Philosophical Transactions of the Royal Society of London A: Mathematical, Physical and Engineering Sciences*, Vol. 179, pp. 43-63.

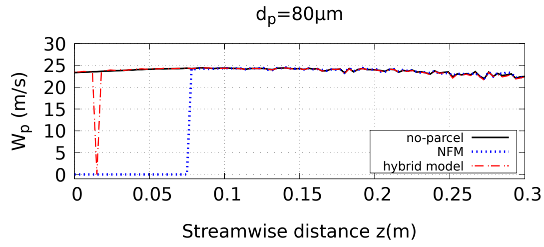

Figure 7: Streamwise profiles of particle mean velocity ($dp = 80\mu m$) for the Hishida configuration comparing no-parcel, NFM and hybrid model.

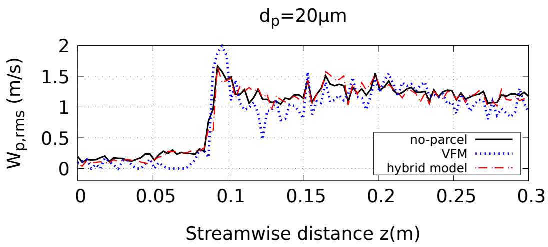

Figure 8: Streamwise profiles of particle RMS velocity ($dp = 20\mu m$) for the Hishida configuration comparing no-parcel, VFM and hybrid model.

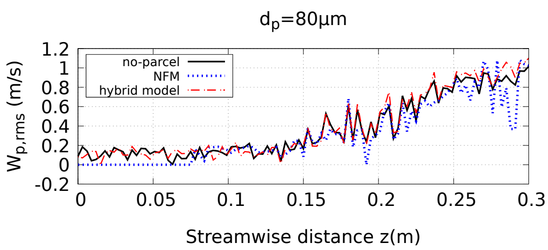

Figure 9: Streamwise profiles of particle RMS velocity ($dp = 80\mu m$) for the Hishida configuration comparing no-parcel, NFM and hybrid model.

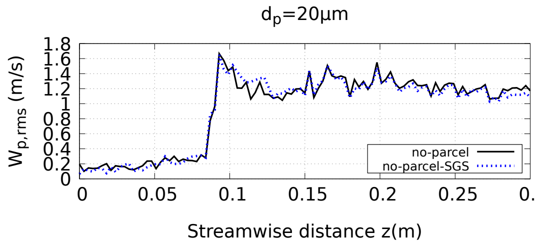

Figure 10: Streamwise profiles of particle RMS velocity ($dp = 20\mu m$) for the Hishida configuration comparing no-parcel model with and without stochastic subgrid model.

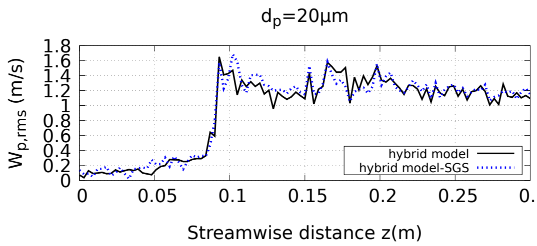

Figure 11: Streamwise profiles of particle RMS velocity ($dp = 20\mu m$) for the Hishida configuration comparing hybrid model with and without stochastic subgrid model.

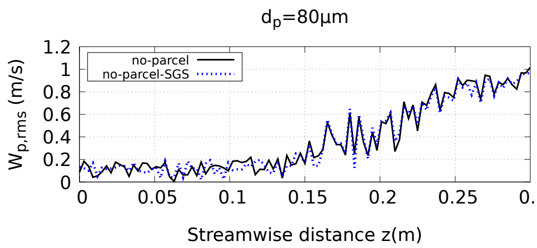

Figure 12: Streamwise profiles of particle RMS velocity ($dp = 80\mu m$) for the Hishida configuration comparing no-parcel model with and without stochastic subgrid model.

Berrouk, A.S. (2012), Stochastic Large Eddy Simulation of an Axisymmetrical Confined-Bluff-Body Particle-Laden Turbulent Flow. *American Journal of Fluid Dynamics*, 2(6), pp. 101-116.

Boussinesq, J. (1885), Sur la resistance qu'oppose un fluide indefini en repos, sans pesanteur, au mouvement varie d'une sphere solide qu'il mouille sur toute sa surface, quand les vitesses restent bien continues et assez faibles pour que leurs carres et produits soient negligiables. *CR Acad. Sc. Paris*, Vol. 100, pp. 935-937.

Bini, M. and Jones, W.P. (2007), Particle acceleration in turbulent flows: A class of nonlinear stochastic models for intermittency *Physics of Fluids*, 19(3).

Bini, M. and Jones, W.P. (2008), Large-eddy simulation of particle-laden turbulent flows *Journal of Fluid Mechanics*, Vol. 614, pp. 207-252.

Fede, P., Simonin, O. (2006), Numerical study of the subgrid fluid turbulence effects on the statistics of heavy colliding particles. *Phys. Fluids*, 18, 045103.

Hishida, K. (1987), Turbulence characteristics of gas-solids two-phase confined jet (effect of particle density) *Japanese Journal of Multiphase Flow*, 1(1), pp. 56-69.

Maxey, M.R. and Riley, J.J. (1983), Equation of motion for a small rigid sphere in a nonuniform flow. *The Physics of Fluids*, 26(4), pp. 883-889.

M. Kuerten, J.G. (2016), t-particle DNS and LES of particle-laden turbulent flow-a state-of-the-art review. *Flow, turbulence and combustion*, 97, pp. 689-713.

Oseen, C.W. (1927), Hydrodynamik. *Akademische Verlagsgesellschaft*.

Sagaut, P. (2005), Large eddy simulation for incompressible flows: an introduction. *Springer Science & Business Media*.

Subramaniam, S. (2013), Lagrangian–Eulerian methods for multiphase flows. *Progress in Energy and Combustion Science*. 39(2-3), pp. 215-245.

Termo Fluids S.L. Termofluids. *http://www.termofluids.com/.*

Trias, F.X., Lehmkuhl, O., Oliva, A., Pérez-Segarra, C.D. and Verstappen, R.W.C.P. (2014), Symmetry-preserving discretization of Navier–Stokes equations on collocated unstructured grids. *Journal of Computational Physics*, 258(1), pp. 246-267.

Watanabe, H., Uesugi, D. and Muto, M. (2015), Effects of parcel modeling on particle dispersion and interphase transfers in a turbulent mixing layer *Advanced Powder Technology*, 26(6), pp. 1719-1728.

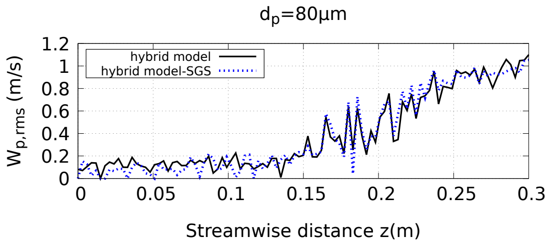

Figure 13: Streamwise profiles of particle RMS velocity ($dp = 80\mu m$) for the Hishida configuration comparing hybrid model with and without stochastic subgrid model.

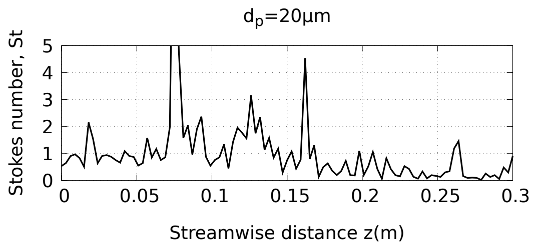

Figure 14: Streamwise profiles of subgrid Stokes number for particle ($dp = 20\mu m$) for the Hishida configuration in no-parcel model without stochastic subgrid model.

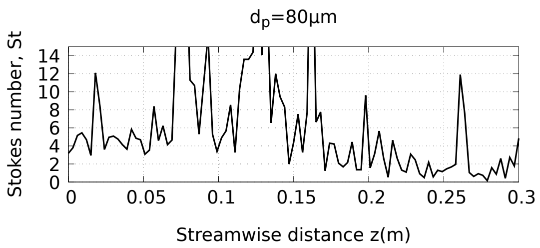

Figure 15: Streamwise profiles of subgrid Stokes number for particle ($dp = 80\mu m$) for the Hishida configuration in no-parcel model without stochastic subgrid model.